

1 **Air pollution measurement errors: Is your data fit for** 2 **purpose?**

3 Sebastian Diez¹, Stuart E. Lacy¹, Thomas J. Bannan², Michael Flynn², Tom Gardiner³, David
4 Harrison⁴, Nicholas Marsden², Nick Martin³, Katie Read^{1,5}, Pete M. Edwards¹

5 ¹Wolfson Atmospheric Chemistry Laboratories, University of York, York, YO10 5DD, UK

6 ²Department of Earth and Environmental Science, Centre for Atmospheric Science, School of Natural Sciences,
7 The University of Manchester, Manchester, M13 9PL, UK

8 ³National Physical Laboratory, Teddington TW11 0LW, UK

9 ⁴Bureau Veritas UK, London, E1 8HG, UK

10 ⁵National Centre for Atmospheric Science, University of York, York, YO10 5DD, UK

11 *Correspondence:*

12 Sebastian Diez (sebastian.diez@york.ac.uk); Pete Edwards (pete.edwards@york.ac.uk)

13 **Abstract.** When making measurements of air quality, having a reliable estimate of the measurement uncertainty
14 is key to assessing the information content that an instrument is capable of providing, and thus its usefulness in a
15 particular application. This is especially important given the widespread emergence of Low Cost Sensors (LCS)
16 to measure air quality. To do this, end users need to clearly identify the data requirements a priori and design
17 quantifiable success criteria by which to judge the data. All measurements suffer from errors, with the degree to
18 which these impact the accuracy of the final data often determined by our ability to identify and correct for them.
19 The advent of LCS has provided a challenge in that many error sources show high spatial and temporal variability,
20 making laboratory derived corrections difficult. Characterising LCS performance thus currently depends primarily
21 on colocation studies with reference instruments, which are very expensive and do not offer a definitive solution
22 but rather a glimpse of LCS performance in specific conditions over a limited period of time. Despite the
23 limitations, colocation studies do provide useful information on measurement device error structure, but the results
24 are non-trivial to interpret and often difficult to extrapolate to future device performance. A problem that obscures
25 much of the information content of these colocation performance assessments is the exacerbated use of global
26 performance metrics (R^2 , RMSE, MAE, etc.). Colocation studies are complex and time-consuming, and it is easy
27 to fall into the temptation to only use these metrics when trying to define the most appropriate sensor technology
28 to subsequently use. But the use of these metrics can be limited, and even misleading, restricting our understanding
29 of the error structure and therefore the measurements' information content. In this work, the nature of common
30 air pollution measurement errors is investigated, and the implications these have on traditional metrics and other
31 empirical, potentially more insightful, approaches to assess measurement performance. With this insight we
32 demonstrate the impact these errors can have on measurements, using a selection of LCS deployed alongside
33 reference measurements as part of the QUANT project, and discuss the implications this has on device end-use.

35 1. Introduction

36 The measurement of air pollutants is central to our ability to both devise and assess the effectiveness of policies
37 to improve air quality and reduce human exposure (Molina & Molina, 2004). The emergence of low-cost sensor
38 (LCS) based technologies means a growing number of measurement devices are now available for this purpose
39 (Morawska et al., 2018), ranging from small low-cost devices that can be carried on an individual's person all the
40 way through to large, expensive reference and research-grade instrumentation. A key question that needs to be
41 asked when choosing a particular measurement technology is whether the data provided is fit for purpose
42 (Andrewes et al., 2021; Lewis & Edwards, 2016). In order to answer this, the user must first clearly define the
43 question that is to be asked of the data, and thus the information required. For example, a measurement to
44 characterize “rush hour” concentrations, or to determine if the concentration of a pollutant exceeded an 8 h average
45 legal threshold value at a particular location would demand a very different set of data requirements than a
46 measurement to determine if a change in policy had modified the average pollutant concentration trend in a
47 neighbourhood. Would the R^2 or RMSE or any other global single-value metric be enough to decide between the
48 different device's options? Considerations such as the origin of the performance data, type of experiment
49 (laboratory or colocation) (Jiao et al., 2016), the test location (Feenstra et al., 2019) and period (i.e. duration,
50 season, etc.), the LCS and reference measurement method (Giordano et al., 2021), measurement time resolution
51 and ability to capture spatial variability (Feinberg et al., 2019) would be important factors to consider for such
52 examples. The measurement uncertainty is also of critical consideration, as this ultimately determines the
53 information content of the data, and hence how it can be used (Tian et al., 2016).

54 All measurements have an associated uncertainty, and even in highly controlled laboratory assessments, the true
55 value is not known, with any measurement error defined relative to our best estimate of the range of possible true
56 values. However, quantifying and representing error and uncertainty is a challenge for a wide range of analytical
57 fields, and often what these concepts represent is not the same to all practitioners. This results in a spectrum of
58 definitions that take into account the way truth, error, and uncertainty are conceived (Grégis, 2019; Kirkham et
59 al., 2018; Mari et al., 2021). For atmospheric measurements assessing uncertainty is complex and non-trivial.
60 Firstly, given the “true” value can never be known, an agreed reference is needed. Secondly, the constantly
61 changing atmospheric composition means that repeat measurements cannot be made and the traditional methods
62 for determining the random uncertainty are not applicable. And finally, a major challenge arises from the multiple
63 sources of error both internal and external to the sensor that can affect a measurement. Signal responses from a
64 non-target chemical or physical parameter or electromagnetic interference are examples of an almost limitless
65 number of potential sources of measurement error. In this work, we will follow the definitions given by the
66 International Vocabulary of Metrology (JCGM, 2012) for measurement error (“measured quantity value minus a
67 reference quantity value”) and for measurement uncertainty (“non-negative parameter characterising the
68 dispersion of the quantity values being attributed to a measurand, based on the information used”). Also, when
69 the term “uncertainty” is used here, it is referring to “diagnosis uncertainty”, in contrast with “prognosis
70 uncertainty” (see Sayer et al. 2020 for more details).

71 The covariance of many of the physical and chemical parameters of the atmosphere, makes accurately identifying
72 particular sources of measurement interference or error very difficult in the real world. Unfortunately, specific
73 laboratory experiments for the characterization of errors is complex and very expensive, resulting in many sources
74 of error being essentially unknown for many measurement devices. The use of imperfect error correction
75 algorithms that are not available to the end-user (e.g. in many LCS devices) makes error identification and
76 quantification even more complex. For this reason, colocation experiments in relevant environments are often the
77 best option to assess the applicability of a given measurement method for its intended purpose.

78 The mentioned difficulties in defining and quantifying uncertainty across the full range of end-use applications of
79 a measurement device, means that often the quoted measurement uncertainty is not applicable, or in some cases
80 not provided or provided in an ambiguous manner. This makes assessing the applicability of a measurement device
81 to a particular task difficult for users. In this work, we investigate the nature of common air pollution measurement
82 errors, and the implications these have on traditional goodness-of-fit metrics and other, potentially more insightful
83 approaches to assess measurement uncertainty. We then use this insight to demonstrate the impact these errors
84 can have on measurements, using a selection of LCS deployed alongside reference measurements as part of the
85 UK Clean Air program funded QUANT (Quantification of Utility of Atmospheric Network Technologies) project,
86 a 2-year colocation study of 26 commercial LCS devices (56 gases measurements and 56 PM measurements) at
87 multiple urban, background and roadside locations in the UK. After analysing some of the real-life uncertainty
88 characteristics we discuss the implications this has on data use.

89 **2. Error characterization**

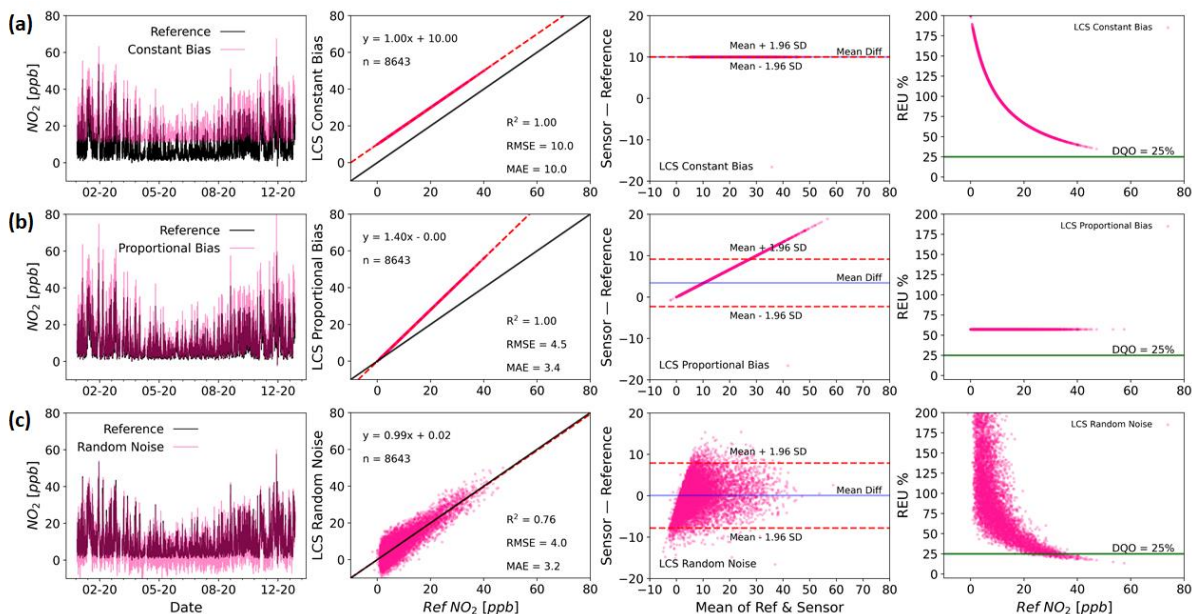
90 When characterising measurement error, in the absence of evidence to the contrary a linear additive model is often
91 assumed. Once the analytical form of the model is defined, its parameters aim to capture the error characteristics,
92 and in the case of linear models (Eq. (1)), these are typically separated into three types (Tian et al., 2016): (i)
93 proportional bias or scale error (b_1), (ii) constant bias or displacement error (b_0) and (iii) random error (ε) (Tian et
94 al., 2016). Any measurement (y_i , e.g from the LCS) can therefore be thought of as a combination of the reference
95 value (x_i) and the three error types, such that:

$$96 \quad y_i = b_1 x_i + b_0 + \varepsilon \quad (1)$$

97 As the simplest approximation, this linear relationship for the error characteristics is often used to correct for
98 observed deviations between measurements and the agreed reference. It is worth to note, however, that this
99 equation assumes time-independent error contributions and that the three error components are not correlated,
100 which is often not the case on both counts (e.g. responses to non-target compounds). The parameter values
101 determined for Eq. (1) are also generally only applicable for individual instruments, potentially in specific
102 environments, unless the transferability of these parameters between devices has been explicitly demonstrated.

103 Figure 1 shows examples of how pure constant bias (a-panels), pure proportional bias (b-panels), and pure random
104 noise (c-panels) would look like in time-series, regression, Bland-Altman (B-A) (Altman & Bland, 1983) and
105 Relative Expanded Uncertainty (REU, as defined by the GDE (2010)) plots. In each of these ideal cases, the error
106 plots enable the practitioner to view the error characteristics in slightly different ways, allowing the impacts of the
107 observed measurement uncertainty to be placed into the context of the data requirements. In this work, we will

108 refer to them as “error types” (in contrast to “error sources”), which is the way they are distilled by the linear error
 109 model.



110
 111 **Figure 1. Time series (left panels), regression (middle-left panels), B-A Bland-Altman (middle-right panels) and REU**
 112 **(right panels, DQO for NO₂ = 25%) plots for arbitrary examples of pure constant bias (Slope = 1, Intercept = 1, SD_ε =**
 113 **0; a-panels), pure proportional bias (Slope = 1.4, Intercept = 0, SD_ε = 0; b-panels) and pure random noise (Slope = 1,**
 114 **Intercept = 0, SD_ε = 4; c-panels) simulated errors.**

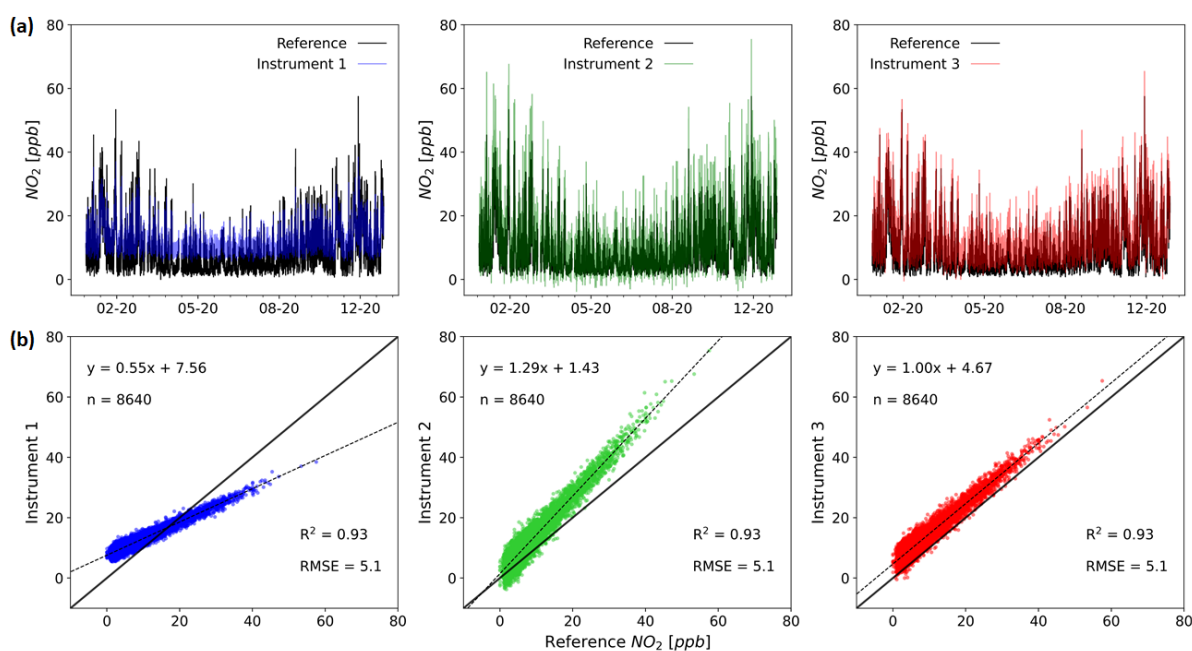
115

116 2.1 Performance indices, error structure and uncertainty

117 A major challenge faced by end-users of measurement devices characterised using collocation studies is the non-
 118 trivial question of how the comparisons themselves are performed and how the data are communicated. Often
 119 single value performance metrics, such as the coefficient of determination (R^2) or root mean squared error
 120 (RMSE), are calculated between the assessed method (e.g. LCS) and an agreed reference, and the user is expected
 121 to infer an expected device performance or uncertainty for a measurement in their application (Duvall et al., 2016;
 122 Malings et al., 2019). When evaluating multiple sensors during a collocation experiment, single metrics can be a
 123 useful way to globally compare instruments/sensors. However, these metrics do little to communicate the nature
 124 of the measurement errors and the impacts these will have in any end use application, in part because they reduce
 125 the error down to a single value (Tian et al., 2016). Furthermore, if a specific concentration range is of paramount
 126 interest to the end-user, these metrics are not capable of characterising the weight of noise and/or the bias effect.
 127 The R^2 shows globally the data set linearity and gives an idea of the measurement noise. However, it is unable to
 128 distinguish whether a specific range of concentrations is more or less linear (or more or less noisy) than another.
 129 Similarly, the RMSE is also a very useful metric and perhaps more complete than R^2 , as it considers both noise
 130 and bias (although they need to be explicitly decomposed from RMSE). Nevertheless, the RMSE is an average
 131 measure (of noise and bias) over the entire dataset under analysis. Using combinations of simple metrics increases
 132 the information communicated, but does not necessarily make it easy to assess how the errors will likely impact

133 a particular measurement application. Visualising the absolute and relative measurement errors across the
134 concentration range (unachievable by global metrics) enables end users to view the errors, and any features (non-
135 linearities, step changes, etc.) that would impact the measurement but that global metrics (and in some cases time-
136 series and/or regression plots) are incapable of showing.

137 Unfortunately, the widespread use of a small number of metrics as the sole method to assess measurement
138 uncertainty, without a thorough consideration of the nature of the measurement errors, means measurement
139 devices are often chosen that are unable to provide data that is fit for purpose. In addition, unconscious about
140 potential flaws, users (e.g. researchers) could communicate findings or guide decision making based on results
141 that may not justify the conclusions drawn from the data. Figure 2 shows three simulated measurements compared
142 with the true values. Despite the measurements having identical R^2 and RMSE values, the time series and
143 regression plots show that the error characteristics are significantly different, and would impact how the data from
144 such a device could viably be used.



145
146 **Figure 2. Time series (a-panels) and regression plots (b-panels) for three hypothetical instruments and a reference (1**
147 **year of data). The most used metrics for evaluating the performance of LCS (R^2 and RMSE) are identical for the**
148 **systems shown, even when the errors have very different characteristics (time res 1 h).**

149 There are multiple performance metrics that can be used for the assessment of measurement errors and uncertainty.
150 Tian et al (2016) present an excellent summary of some of the major pitfalls of performance metrics and promote
151 an approach of error modelling as a more reliable method of uncertainty quantification. These modelling
152 approaches, however, rely on the assumption of statistical stationarity, whereby the statistical properties of the
153 error are constant in the temporal and spatial domains. The presence of unknown or poorly characterised sources
154 of error, for example, due to interferences from other atmospheric constituents or drifts in sensor behaviour, makes
155 this assumption difficult to satisfy, especially when the dependencies of these errors show high spatial and
156 temporal variability. Thus, if field colocation studies are the primary method for performance assessment, as is

157 the case for LCS, only through a detailed assessment of the measurement errors across a wide range of conditions
158 and timescales can the uncertainty of the measurement be realistically estimated.

159 **2.2 Dealing with errors: established techniques vs Low-Cost Sensors**

160 Different approaches are available to the user to minimise the impact of errors, generally by making corrections
161 to the sensor data. For example, in the case of many atmospheric gas analysers, if the error is dominated by a
162 proportional bias, a multi-point calibration can be performed using standard additions of the target gas.
163 Displacement errors can be quantified, and then corrected for, by sampling a gas stream that contains zero target
164 gas. Random errors can be reduced by applying a smoothing filter (e.g moving average filter, time-averaging the
165 data, etc.), at the cost of losing some information (Brown et al., 2008). These approaches work well for simple
166 error sources that, ideally, do not change significantly over timescales from days to months. Unfortunately, more
167 complex error sources can manifest in such a way that they contribute across all three error types, and also vary
168 temporally and spatially. For example, an interference from another gas-phase compound could in part manifest
169 itself as a displacement error, based on the instrument response to its background value, and in part as a
170 proportional bias if its concentration correlates with the target compounds, with any short-term deviations from
171 perfect correlation contributing to the random error component. In this case, time-averaging combined with
172 periodic calibrations and zeros would not necessarily minimise the error, and the user would need to employ
173 different tactics. One option would be to independently measure the interferent concentration, albeit with
174 associated uncertainty, and then use this to derive a correction. This is feasible if a simple and cost-effective
175 method exists for quantifying the interferent and its influence on the result is understood, but can make it very
176 difficult to separate out error sources, and can become increasingly complex if this measurement also suffers from
177 other interferences.

178 For many measurement devices, in particular for LCS based instruments, a major challenge is that the sources and
179 nature of all the errors are unknown or difficult to quantify across all possible end-use applications, meaning
180 estimates of measurement uncertainty are difficult. In the case of most established research and reference-grade
181 measurement techniques, comprehensive laboratory and field experiments have been used to explore the nature
182 of the measurement errors (Gerboles et al., 2003; Zucco et al., 2003). Calibrations have then been developed,
183 where traceable standards are sampled and measurement bias, both constant and proportional, can be corrected
184 for. Interferences from variables such as temperature, humidity, or other gases, have also been identified and then
185 either a solution engineered to minimise their effect or robust data corrections derived. Unfortunately, these
186 approaches have been shown not to perform well in the assessment of LCS measurement errors, due to the
187 presence of multiple, potentially unknown, sensor interferences from other atmospheric constituents (Thompson
188 & Ellison, 2005). These significant sensitivities to constituents such as water vapour and other gases mean
189 laboratory-based calibrations of LCS become exceedingly complex, and expensive, as they attempt to simulate
190 the true atmospheric complexity, often resulting in observed errors being very different to real-world sampling
191 (Rai et al., 2017; Williams, 2020). This has resulted in collocation calibration becoming the accepted method for
192 characterising LCS measurement uncertainties (De Vito et al., 2020; Masson et al., 2015; Mead et al., 2013;
193 Popoola et al., 2016; Sun et al., 2017), where sensor devices are run alongside traditional reference measurement
194 systems for a period of time, and statistical corrections derived to minimise the error between the two. As the true
195 value of a pollutant concentration cannot be known, this collocation approach assumes all the error is in the low-

196 cost measurement. Although this assumption may often be approximately valid (i.e. reference error variance \ll
197 LCS error variance), no measurement is absent of uncertainty and this can be transferred from one measurement
198 to another, obscuring attempts to identify its sources and characteristics. A further consideration when the fast
199 time-response aspect of LCS data is important, is that reference measurement uncertainties are generally
200 characterised at significantly lower reported measurement frequencies (typically 1 hr). This means that a high
201 time-resolution (e.g. 1 min) reference uncertainty must be characterised in order to accurately estimate the LCS
202 uncertainty (requiring specific experiments and additional costs). If a lower time-resolution reference data set is
203 used as a proxy, then the natural variability timescales of the target compound should be known and any impact
204 of this on the reported uncertainty caveated.

205 Another challenge with this approach is that, unlike targeted laboratory studies, real-world colocation studies at a
206 single location, and for a limited time period, are not able to expose the measurement devices to the full range of
207 potential sampling conditions. As many error sources are variable, both spatially and temporally, using data
208 generated under a limited set of conditions to predict the uncertainty on future measurements is risky. Deploying
209 a statistical model makes the tacit assumption that all factors affecting the target variable are captured by the
210 model (and the data set used to build the model). This is very often an unrealistic demand, and in the complex
211 multifaceted system that is atmospheric chemistry, this is extremely unlikely to be tenable, resulting in a clear
212 potential for overfitting to the training dataset. Ultimately, however, these colocation comparisons with
213 instruments with a well-quantified uncertainty need to be able to communicate a usable estimate of the information
214 content of the data to end-users, so that devices can be chosen that are fit for a particular measurement purpose.

215 **3. Methods**

216 In this work, we explore measurement errors, and their impacts, using the most common single value metrics: the
217 Coefficient of Determination or R^2 , the Root Mean Squared Error or RMSE and the Mean Absolute Error or MAE
218 (see the equation definitions in Cordero et al., 2018). To visualise the error distribution across a dataset we have
219 also employed two additional widely used approaches: the Bland-Altman plots (B-A) and Relative Expanded
220 Uncertainty (REU).

221 The performance metrics provide a single value irrespective of the size of the dataset, and might appear convenient
222 for users when comparing across devices or datasets, but can encourage over-reliance on the metric, often at the
223 expense of looking at the data in more detail or bringing an awareness of the likely physical processes driving the
224 error sources. On the other hand, the use of visualisations such as B-A and REU is complementary to the
225 aforementioned metrics, with the added value that the user is now more aware of how the data looks like in an
226 absolute and/or relative error space, allowing them to distinguish some characteristics of interest. These
227 visualizations are indeed more laborious and the interpretation can be challenging for non-experts, but they
228 provide additional insights into the nature of the errors, not attainable by one or more combined performance
229 metrics: while B-A plots shows the noise (dispersion of the data) and the bias effect (tendency of the data) in an
230 absolute scale, the REU can be explicitly decomposed in the noise and bias components (see Yatkin et al., 2022).

231 In order to understand how the different tools used here show different characteristics of the error structure, some
232 errors commonly found in LCS are examined through simulation studies. Subsequently, two real world case

233 studies are presented: (i) LCS duplicates for NO₂ and PM_{2.5} belonging to the QUANT project located in two sites
234 -the Manchester Natural Environment Research Council (NERC) measurement Supersite, and the York Fishergate
235 Automatic Urban and Rural Network (AURN) roadside site- and (ii) a set of duplicate reference instruments (only
236 at Manchester Supersite). Table S1 shows the research grade instrumentation used for this study.

237 3.1 Visualisation tools

238 An ideal performance metric should be able to deliver not only a performance index but also an idea of the
239 uncertainty distribution (Chai & Draxler, 2014). This is difficult to deliver through a simple numerical value, and
240 easy to interpret visualisations of the data are often much more useful for conveying multiple aspects of data
241 performance. Figure 2 shows the two most common data visualisation tools, the time-series plot and the regression
242 plot. In the time series plot the instrument under analysis and the agreed reference are plotted together as a function
243 of time. This allows a user to visually assess tendencies of over or under prediction, differences in the base line
244 or other issues, but can be readily over interpreted and does not allow for easy quantification of the observed
245 errors. In the regression plot the data from the instrument under analysis is plotted against the agreed reference
246 data. This allows for the correlation between the two methods to be more readily interpreted, in particular any
247 deviations from linearity, but gives little detail on the nature of the errors themselves.

248 In contrast to the regression plot -where the measured values from the two measurements (e.g. LCS vs Ref) are
249 plotted against each other- the Bland-Altman plots essentially display the difference between measurements
250 (abscissa) as a function of the average measurement (ordinate), enabling more information on the nature of the
251 error to be communicated. This direct visualisation of the absolute error acknowledges that the true value is
252 unknown and that both measurements have errors. The B-A plot enables the easy identification of any systematic
253 bias between the measurements or possible outliers, and is the reason B-A plots are extensively used in analytical
254 chemistry and biomedicine to evaluate agreement between measurement methods (Doğan, 2018). The mean
255 difference between the measurements, represented by the blue line in the figures, is the estimated bias between
256 the two observations. The spread of error values around this average line indicates if the error shows purely
257 random fluctuations around this mean, or if it has structure across the observed concentration range.

258 In the case where all the error is assumed to be in one of the measurements, e.g. comparing a LCS to a reference
259 grade measurement, there is an argument that the B-A abscissa could be the agreed reference value instead of the
260 average of two measurements. However, in this work we use the average of the two values as per the traditional
261 B-A analysis. To illustrate the B-A interpretation, from the error model (Eq. (1)) we can derive the following
262 expression:

$$263 \quad y_i - x_i = x_i (b_1 - 1) + b_0 + \varepsilon \quad (2)$$

264 From Eq. (2) it can be seen that if $b_1 \neq 1$ or if the error term (ε) variance is non-constant (e.g. heteroscedasticity)
265 the difference will not be normally distributed. The B-A plot (with x_i as the reference instrument results) allows a
266 quick visual assessment of the error distribution without the need to calculate the model parameters. In the case
267 the differences are normally distributed, the so-called “agreement interval” (usually defined as $\pm 2\sigma$ around the
268 mean) will hold 95% of the data points. Even though the estimated limits of agreement will be biased if the

269 differences are not normally distributed, it can still be a valuable indicator of agreement between the two
270 measurements.

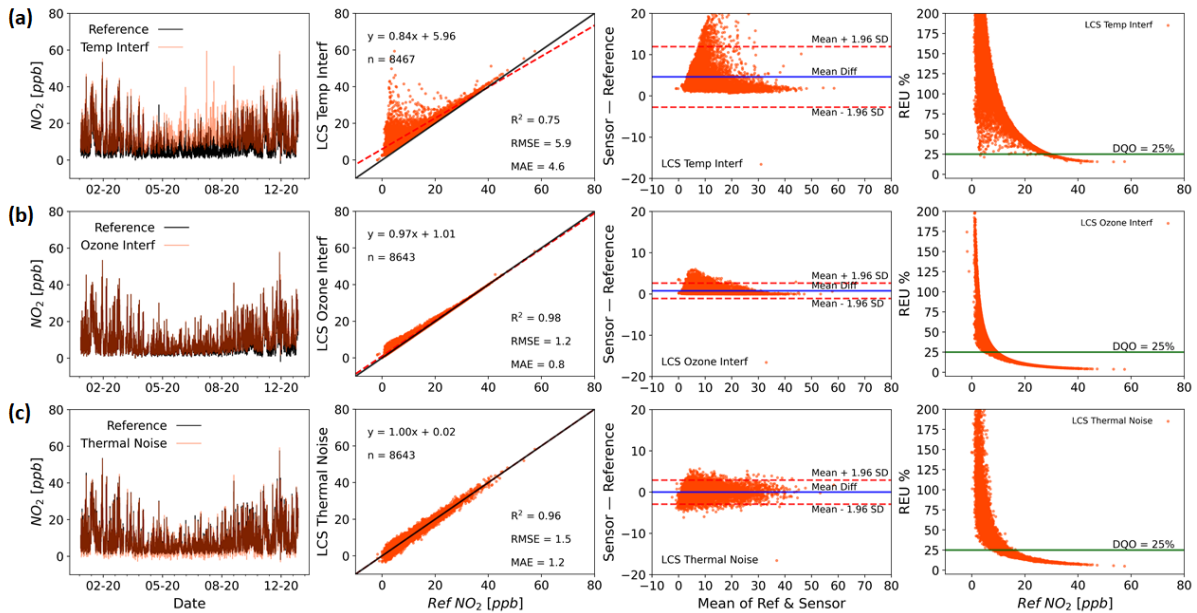
271 If the ultimate goal of studying measurement errors is to diagnose the measurement uncertainty in a particular
272 target measurement range, then visualising the uncertainty in pollutant concentration space can be very
273 informative. The REU provides a relative measure of the uncertainty interval about the measurement within which
274 the true value can be confidently asserted to lie. The abscissa in an REU plot represents the agreed reference
275 pollutant concentration, whose error is taken into account, something not considered by the other metrics or
276 visualisations discussed. The REU is regularly used to assess measurement compliance with the Data Quality
277 Objective (DQO) of the European Air Quality Directive 2008/50/EC, and is mandatory for the demonstration of
278 equivalence of methods other than the EU reference methods. For LCS the REU is widely used as a performance
279 indicator (Bagkis et al., 2021; Bigi et al., 2018; Castell et al., 2017; Cordero et al., 2018; Spinelle et al., 2015).
280 However, the evaluation of this metric is perceived as arduous and cumbersome and it is not included in the
281 majority of sensor studies (Karagulian et al., 2019). There is now a new published European Technical
282 Specification (TS) for evaluating the LCS performance for gaseous pollutants (CEN/TS 17660-1:2021). It
283 categorises the devices in 3 classes according to the DQO (Class 1 for “indicative measurements”, Class 2 for
284 “objective estimations”, and Class 3 for non-regulatory purposes, e.g. research, education, citizen science, etc.).
285 In the following sections, we use these established methods for assessing measurement uncertainty, alongside
286 simple time series and regression plots, to explore different error sources and their implications for air pollution
287 measurements.

288 **4. Case studies**

289 **4.1 Simulated instruments**

290 In order to investigate the impact of different origins of measurement error on measurement performance, a set of
291 simulated datasets have been created. These data are derived using real-world reference data as the true values,
292 with the subsequent addition of errors of different origins to generate the simulated measurement data. Error
293 origins were chosen for which examples have been described in the LCS literature. Performance metrics along
294 with visualisation methods are then used to assess measurement performance.

295 As the complexity of the error increases, the impact of the assumption of statistical stationarity can become more
296 difficult to satisfy, with the magnitude of the errors becoming less uniform across the observed concentration, and
297 hence spatial, or time domains. Figure 3 shows examples of modelled sources of errors on NO₂ measurements:
298 temperature interference (correction model taken from (Popoola et al., 2016), a-panels), a non-target gas (ozone)
299 interference (correction model taken from (Peters et al., 2021), b-panels) and thermal electrical noise (white noise,
300 c-panels).



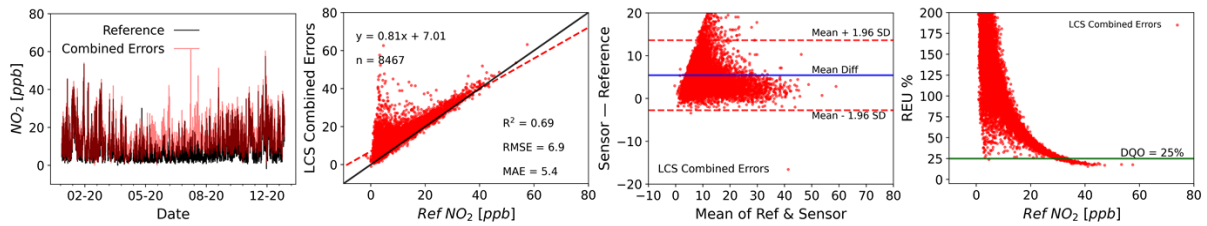
301

302 **Figure 3. Time series (left panels), regression plots (middle-left panels, including R^2 , RMSE & MAE), Bland-Altman**
 303 **plots (middle-right panels) and REU (right panels, DQO for $\text{NO}_2 = 25\%$) for temperature (a-panels), ozone (b-panels)**
 304 **and thermal electrical noise (c-panels) modelled interferences on NO_2 measurements (time res 1 h).**

305 The above simulations show examples of how individual sources of error can impact measurement performance.
 306 Figure S1 shows some more examples, this time for different drift effects (baseline drift, temperature interference
 307 drift and instrument sensitivity drift). This set of error origins is not exhaustive, with countless others potentially
 308 impacting the measurement, such as those coming from (i) hardware (sensor-production variability, sampling,
 309 thermal effects due to materials expansion, drift due to ageing, RTC lag, Analog-to-Digital conversion,
 310 electromagnetic interference, etc.), (ii) software (signal sampling frequency, signal-to-concentration conversion,
 311 concept drift, etc.), (iii) sensor technology/measurement method (selectivity, sensitivity, environmental
 312 interferences, etc.) and (iv) local effects (spatio-temporal variation of concentrations, turbulence, sampling issues
 313 etc.).

314 Each error source impacts the uncertainty of the measurement, which in turn impacts its ability to provide useful
 315 information for a particular task. For example, the form of the temperature interference shown in Fig. 3 (a-panels)
 316 results in the largest errors being seen at the lower NO_2 values. This is because NO_2 concentrations are generally
 317 lowest during the day, due to photolytic loss when temperatures are highest. Thus, this device would be better
 318 suited to an end-user intending to assess daily peak NO_2 concentration compared with the daytime hourly exposure
 319 values, providing the environment the device was deployed in showed a similar relationship between temperature
 320 and true NO_2 as that used here. The O_3 interference shown in Fig. 3 (b-panels) is similar, due again to a general
 321 anti-correlation observed between ambient O_3 and NO_2 concentrations. This type of interference can often be
 322 interpreted incorrectly as a proportional bias, and a slope correction applied to the data. However, this type of
 323 correction will ultimately fail as O_3 concentrations are dependent on a range of factors, such as hydrocarbon
 324 concentrations and solar radiation, and as these change the O_3 concentration relative to the NO_2 concentration will
 325 change. To further complicate matters, multiple error sources can act simultaneously, meaning that the majority

326 of measurements will contain multiple sources of error. Figure 4 shows a simple linear combination of the
327 modelled errors shown in Fig 3, and the impact this has on the performance metrics.



328
329 **Figure 4. Time series (left panel), regression plot (middle-left panel, including R^2 , RMSE & MAE), Bland-Altman**
330 **plot (middle-right panel) and REU (right panel, DQO for $\text{NO}_2 = 25\%$) for a linear combination of temperature, ozone**
331 **and thermal electrical noise modelled interferences (time res 1 h).**

332 As the simulations show, the nature of the errors determines the observed effect on the measurement performance.
333 In an ideal situation, like those shown in figures 3 and 4, the error sources would be well characterised, allowing
334 the error to be modelled and approaches such as calibrations (for bias) and smoothing (for random errors)
335 employed to minimise the total uncertainty. Unfortunately, in scenarios where sources of error and their
336 characteristics are not known, modelling the error becomes more difficult and a more empirical approach to
337 assessing the measurement performance and uncertainty may be required. The growing use of LCS represents a
338 particular challenge in this regard. The susceptibility of LCS to multiple, often unknown or poorly characterised,
339 error sources means that in order to determine if a particular LCS is able to provide data with the required level
340 of uncertainty for a given task, a relevant uncertainty assessment is required. The following section explores the
341 uncertainty characteristics of several LCS, with unknown error sources, deployed alongside reference
342 instrumentation in UK urban environments as part of the QUANT study.

343 4.2 Real-world instruments

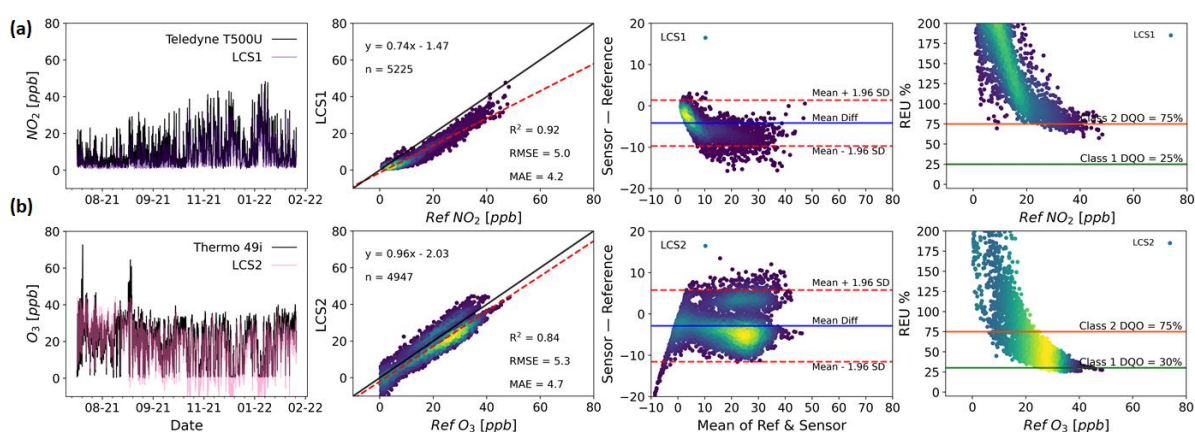
344 The difficulty in generating representative laboratory error characterisation data means for many measurement
345 devices the error sources are essentially unknown. This, combined with the use of imperfect algorithms that are
346 not available to the end-user (i.e. “black-box” models) to minimise errors, means that, collocation data is often the
347 best option available to end-users in order to assess the applicability of a measurement method for their desired
348 purpose. This is particularly the case for LCS air pollution measurement devices. In this section, we show
349 collocation data collected as part of the UK Clean Air program funded QUANT project, and use the tools described
350 above to investigate the impact of the observed errors on end-use.

351 Figure 5 shows two collocated measurements from two different LCS devices: one measuring NO_2 (a-panels) and
352 the other O_3 (b-panels). Both measurements are compared with collocated reference measurements at an urban
353 background site in the city of Manchester. Unlike the modelled instruments in Sect. 4.1, the combination of error
354 sources is unknown in this case, and we can thus only assess the LCS measurement performance through
355 comparison with the reference measurements using global metrics and visual tools.

356 Single value metrics indicate an acceptable performance for both measurements: high linearity (both R^2 are higher
357 than 0.8) and relatively low errors (RMSE ~ 5 ppb). However, the plots present the data in a variety of ways that
358 enable the user to identify patterns in the measurement errors that would be less obvious if only global metrics

359 were used. For example, the NO₂ sensor (LCS1, a-panels) has a non-linear response that is almost imperceptible
 360 from the regression plot but stands out in the B-A plot. Furthermore (despite the high R² and relatively low
 361 RMSE), the REU plot shows high relative errors that do not meet the Class 2 DQO for the measured concentration
 362 range. Regarding the O₃ sensor (LCS2, b-panels), the B-A plot shows two high density measurement clusters, one
 363 with positive absolute errors (over-measuring) and a larger one with negative errors (under-measuring). These are
 364 the result of a step change in the correction algorithm applied by the manufacturer and could easily have been
 365 missed if only summary metrics and a regression plot were used, especially if the density of the data points was
 366 not coloured.

367 It is worth noting that these plots do not directly identify the source of the proportional bias, with sensor response
 368 to the target compound or another covarying compound possible, but provide information on how much it impacts
 369 the data.



370
 371 **Figure 5. Time series (left panels), regression plots (middle-left panels), Bland-Altman plots (middle-right panels) and**
 372 **REU (right panels; NO₂ Class 1 DQO = 25% & Class 2 DQO = 75% ; O₃ Class 1 DQO = 30% & Class 2 DQO = 75%)**
 373 **for NO₂ (a-panels) and O₃ (b-panels) measurements by two LCS systems of different brands in the same location and**
 374 **time span (Manchester Supersite, July 2021 to February 2022. Time res 1 h). All but the time-series plots, have been**
 375 **coloured by data density (darker colours denote lower density and lighter colours denote higher density).**

376
 377 Figure 6 shows three out-of-the-box PM_{2.5} measurements made by two devices (LCS3 & LCS4) from the same
 378 brand in spring (LCS3: a-panels; LCS4: c-panels) and in autumn (b-panels, only LCS3). The colocation shown
 379 corresponds to two different sites: an urban background site (LCS3, a and c-panels) and a roadside site (LCS4, c-
 380 panels).

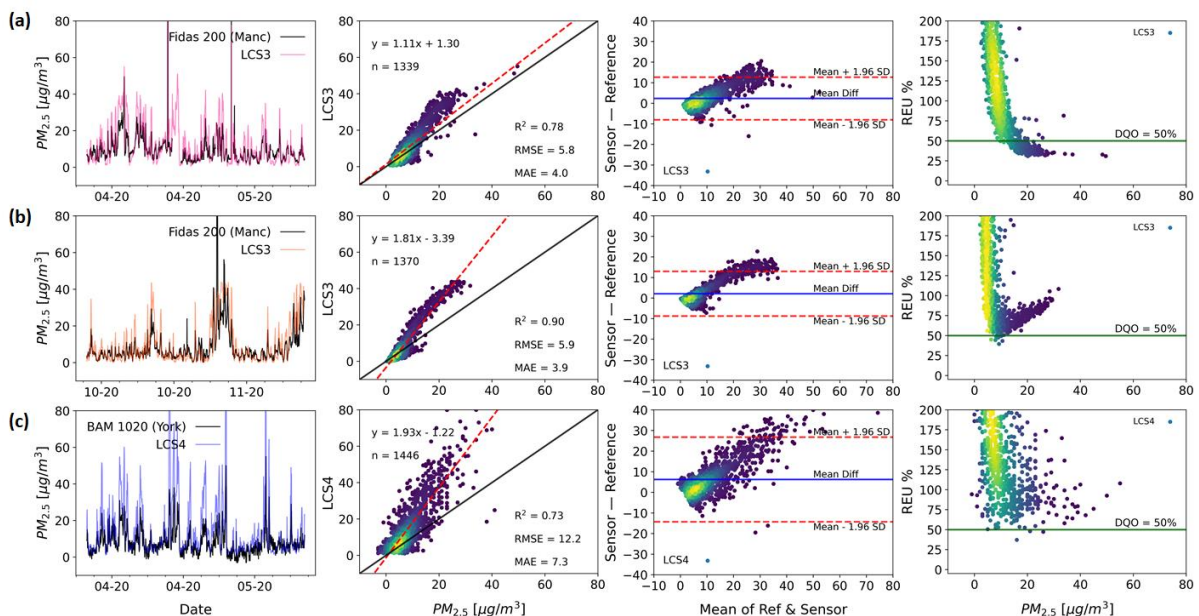
381 As the regression and the B-A plots show, all LCS measurements in Fig. 6 have a proportional bias compared
 382 with the reference, with the LCS over predicting the reference values. The device at the urban background site
 383 (LCS3) show a dissimilar performance in spring and autumn, indicating that the errors this device suffers are
 384 differently influenced by local conditions in the two seasons (all the duplicates at the urban background show the
 385 same pattern). While for LCS3 during spring the error have a more linear behaviour, in autumn a non-linear pattern
 386 is clearly observed in the regression and B-A plots. Despite the utility that single metrics can have in certain

387 circumstances, the non-linear pattern goes completely unnoticed by them: while for the two different seasons
 388 RMSE and the MAE are almost constant the R^2 indicates a higher linearity for autumn.

389 A number of duplicates were deployed at both sites showing a very similar performance in terms of the single
 390 metric values but also in regard to the more visual tools (not shown here). This internal consistency is highly
 391 desirable, especially when LCS's are to be deployed in networks, as although mean absolute measurement error
 392 may be high, differences between identical devices are likely to be interpretable.

393 Having prior knowledge of the nature of the measurement errors allows informed experimental design prior to
 394 data collection. This is key if an end user is to maximise the power of a dataset, and the information it provides,
 395 to answer a specific question. For example, if an end-user wanted to identify pollution hotspots within a relatively
 396 small geographical area, then using a dense network of sensor devices that possess errors with both sufficiently
 397 large magnitude and variance to make quantitative comparisons with limit values difficult (possibly due to an
 398 interference from a physical parameter like relative humidity) but show internal consistency could be a viable
 399 option, providing the hotspot signal is large enough relative to any random error magnitude.

400



401
 402 **Figure 6. Two LCS systems (LCS3 & LCS4, same brand) measuring $PM_{2.5}$ (Time res 1 h). While LCS3 is shown for the**
 403 **same location (Manchester) but unfolded in two different seasons (a-panels: Apr to May 2020; b-panels: Oct to Nov**
 404 **2020), LCS4 is at a different location (c-panels: York, Apr to May 2020). Time series (left panels), regression plots**
 405 **(middle-left panels), Bland-Altman plots (middle-right panels) and REU (right panels; $DQO_{PM_{2.5}} = 50\%$) are used to**
 406 **characterise the device's error structure. All but the time-series plots have been coloured by data density (darker**
 407 **colours denote lower density and lighter colours denote higher density).**

408

409 The LCS data from the roadside location (LCS4) show significantly lower precision than those at the urban
 410 background site, as seen in the B-A plot. This could be caused by differences in particle properties and size

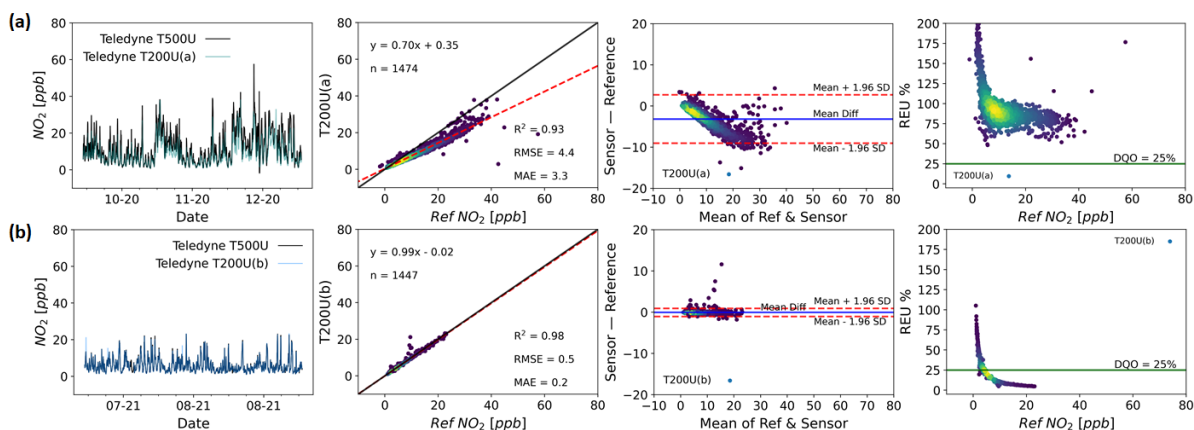
411 distributions between the two sites (Gramsch et al., 2021), and by the high frequency variation of transport
412 emissions close to the roadside site and turbulence effects (Baldauf et al., 2009; Makar et al., 2021). Duplicate
413 measurements show that all sensors of this type responded similarly in this roadside environment (not shown
414 here), supporting the high internal consistency of this device, but indicating a spatial heterogeneity in some key
415 error sources. It is also worth noting that the gold standard instruments at the two sites are not “reference method”
416 but “reference equivalent methods” (GDE, 2010), each using a different measurement technique: while an optical
417 spectrometer (Palas Fidas 200) is used in Manchester, the York instrument uses a Beta attenuation method (Met
418 One BAM 1020), which could also potentially lead to some of the observed differences. The increased apparent
419 random variability for LCS4, combined with the proportional bias, results in significantly higher measurement
420 uncertainty across the observed range, as can be seen by the REU plots, with LCS4 never reaching an acceptable
421 DQO level (50% for $PM_{2.5}$). If the observed proportional bias is corrected the linearly bias-corrected sensors (Fig.
422 S3) show a much-improved comparison with the reference measurement, specially LCS3* in autumn and LCS4*
423 (the asterisk is to indicated the LCS has been bias corrected). The error distribution for the LCS3 (autumn) shown
424 by the B-A plot is greatly narrowed (~ 3 times) and now the sensor is accomplishing the DQO below $10 \mu g m^{-3}$ as
425 the REU plot indicates. For LCS4 the B-A plot shows an error characteristic more dominated by random errors,
426 and a significant reduction of the relative uncertainty, with the REU at $10 \mu g m^{-3}$ reducing from ~ 75 to $\sim 50\%$.

427 As a comparison for the LCS data shown above, Fig. 7 shows two identical NO_2 reference grade instruments,
428 Teledyne T200U (Chemiluminescence method) at the Manchester urban background site (panels a and b) during
429 two different time periods, with a Teledyne T500U (CAPS detection method) used as the “ground truth”
430 instrument. Instrument “a” manifests a significant proportional bias, in contrast to instrument “b”, but both show
431 differences that could be non-negligible depending on the application. The deviations observed in instrument “a”
432 was due to the cell pressure being above specification by $\sim 20\%$, unnoticed while the instrument was in operation.
433 This demonstrates the importance of checking instrument parameters regularly in the field even if the data appears
434 reasonable.

435 As the LCS error structure is determined relative to the performance of a reference measurement, if the reference
436 instrument suffers from significant errors this will affect the outcomes of the performance assessment, due to the
437 assumption that all the errors reside with the LCS. As Fig. 7 shows, however, this assumption is not necessarily
438 always valid and potentially argues that reference instruments used in colocation studies should be subject to
439 further error characterisation, including possible colocation with other reference instruments. As a similar
440 comparison of reference instruments, Fig. S3 shows two ozone research grade instruments (a Thermo 49i and a
441 2B).

442 It is worth noting that even when using reference, or reference equivalent, grade instrumentation, inherent
443 measurement errors mean that relative uncertainty, as shown in the REU plot, increases asymptotically at lower
444 values. This is not unexpected, but is potentially important as ambient target concentration recommendations
445 continue to fall based on updated health evidence (World Health Organization, 2021).

446



447
 448 **Figure 7. Time series (left panel), regression plots (middle-left panel), Bland-Altman plots (middle-right panel) and**
 449 **REU (right panel, DQO for NO₂ = 25%) for two identical (Teledyne T200U) reference NO₂ instruments (panels a and**
 450 **b) colocated at the Manchester Supersite (1h time res). The first instrument between October & November 2020 and**
 451 **the second between July & August 2021. All but the time-series plots have been coloured by data density (darker colours**
 452 **denote lower density and lighter colours denote higher density).**

453 **5. Discussion**

454 The widespread use of colocation studies to assess measurement device performance, means many examples exist
 455 in the LCS literature where different devices are compared using summary metrics for field or laboratory studies
 456 (Broday, 2017; Duvall et al., 2016; Hofman et al., 2022; Karagulian et al., 2019; Mueller et al., 2017; Rai et al.,
 457 2017; van Zoest et al., 2019). Although these comparisons do provide useful information, they can be misleading
 458 for end users wanting to compare the performance of different devices, as they are often carried out under different
 459 conditions and do not present the data or experimental design in full. Even in the case where comparisons have
 460 been done under identical conditions, the data still needs to be treated with caution, as inevitable differences
 461 between assessment environment and proposed application environment, as well as any changes to
 462 instrument/sensor design or data processing, mean that past performance does not guarantee future performance.

463 All measurement devices suffer from measurement errors, many of which are potentially significant depending
 464 on the application, with devices and their error susceptibility covering a broad spectrum. As evidenced by Fig. 7,
 465 reference instruments are not immune from these phenomena, with the proportional bias of one of the NO_x
 466 instruments clearly affecting its measurements resulting in the absolute error increasing with concentration. As
 467 the requirements on measurement devices continue to increase, driven in part by new evidence supporting the
 468 reduction of air pollutant target values, the devices currently being used for a particular application could no longer
 469 be fit-for-purpose in the situation where the limit value has decreased to the point where it is small relative to the
 470 device's uncertainty.

471 Single value performance metrics, such as R² and RMSE, can seem convenient when comparing multiple co-
 472 located devices as they facilitate decision making when a threshold criterion is defined. However, these scalar
 473 values hide important information about the scale and / or distribution of the errors within a dataset; graphical
 474 summaries of the measurements themselves can offer significantly more insight into the impact of measurement
 475 errors on device performance and ultimate capabilities. Of particular use in air pollution measurements is the
 476 ability to see how the errors manifest themselves in relation to our best estimate of the true pollutant concentration,

477 as often applications have specific target pollutant concentration ranges of interest. For example, the two LCS
478 devices shown in Fig. 5 have considerably high R^2 values (0.92 and 0.84) and relatively low RMSE and MAE,
479 but one suffering of non-linear errors (LCS1) and the other with data coming from two different calibration states
480 (LCS2).

481 Errors, or combinations of errors, frequently result in varying magnitude of the observed measurement
482 inaccuracies across the concentration space observed, and it is often useful to assess both the absolute and relative
483 effects of the errors. By getting a more complete picture of the device performance, decisions can be made on the
484 effectiveness of simple corrections, such as correcting for an apparent proportional bias using an assumption of a
485 linear error model. Ultimately end users need to identify the data requirements a priori and design quantifiable
486 success criteria by which to judge the data. For example, rather than just wanting to measure the 8-hour average
487 NO_2 , be more specific and require that this needs to be accurate to within 5 ppb, have demonstrated approximately
488 normally distributed errors in a representative environment for the period of interest, and no statistical evidence
489 of deviation from a linear correlation with the reference measurement over the target concentration range for the
490 period of interest.

491 A major challenge comes from complex errors, such as interferences from other compounds or with environmental
492 factors, that vary temporally and/or spatially. Similar graphical techniques to those presented above can be used
493 to identify the existence of such relationships, but correcting for them remains a challenge. For example, the
494 correlation between measurement errors and relative humidity could be explored by replacing the abscissa with
495 measured relative humidity in both the B-A and REU plots. This would visualise the relationship between absolute
496 and relative errors with relative humidity, but would not be able to confirm causality. The complex and covarying
497 nature of the atmosphere means that the best way to identify a device error source is through controlled laboratory
498 experiments, where confounding variables can be controlled, although these experiments are often difficult and
499 expensive to perform in a relevant way.

500 This brings into question the power of colocation studies, as they can ultimately never be performed under the
501 exact conditions for every intended application. The $\text{PM}_{2.5}$ sensors shown in Fig. 6 demonstrate this, as if a
502 colocation dataset generated at the urban background site was used to inform a decision about the applicability of
503 these devices to a roadside monitoring task, then an overly optimistic assessment of the scale of the errors to be
504 expected would be likely. It is therefore always desirable that colocation studies are as relevant as possible to the
505 desired application, and this is even more paramount in the case where the error sources are poorly specified. For
506 this reason, complete meta-data on the range of conditions over which a study was conducted is key information
507 in judging its applicability to different users.

508 Although there is no strict definition on what makes a device a LCS, we often make the categorization based on
509 the hardware used. Standard reference measurement instruments are generally based on well-characterised
510 techniques developed and improved over years, based primarily on the progressive refinement of hardware (e.g.
511 materials used for the detection elements, electronic circuits to filter noise, refinement of production methods,
512 etc.). Although LCS sensor technologies are improving, it is interesting that many of the significant improvements
513 that have been made to LCS performance have been through software, rather than hardware advances. As more
514 colocation data are generated in different environments, many LCS manufacturers have been able to develop data

515 correction algorithms that minimise the scale of the errors that are present on the LCS hardware. This can greatly
516 improve the performance of LCS devices, and has been a large factor in the improvements seen in these devices
517 over recent years. These algorithms are, however, inevitably imperfect and can suffer from concept drift (De Vito
518 et al., 2020), caused by the lack of available colocation data over a full spectrum of atmospheric complexity.
519 Furthermore, any kind of statistical model introduces a new error source that can work in conjunction with the
520 pre-existing measurement errors to drastically change the observed error characteristics, making it much more
521 difficult for users to interpret and extrapolate from colocation study performance to intended application. If end
522 users are to be able to make well informed decisions about device applicability, then information on the scale of
523 the measurement errors, and the impact of corrections made to minimise these, should be made available.
524 Exemplar case studies in a range of relevant environments would also be highly valuable. Unfortunately, this
525 colocation data are costly to generate, meaning relevant data often does not exist, and when it does is often not
526 communicated in such a way that enables the user to make a fully informed decision.

527 **6. Conclusions**

528 In situ measurements of air pollutants are central to our ability to identify and mitigate poor air quality.
529 Measurement applications are wide ranging, from assessing legal compliance to quantifying the impact of an
530 intervention. The range of available measurement tools for key pollutants is also increasingly broad, with
531 instrument price tags spreading several orders of magnitude. In order for a measurement device to be of use for a
532 particular application it must be fit-for-purpose, with cost, useability and data quality all needing to be considered.
533 Understanding measurement uncertainty is key in choosing the correct tool for the job, but in order for this to be
534 assessed the job needs to be fully specified a priori. The specific data requirements of each measurement
535 application need to be understood and a measurement solution chosen that is capable of providing data with
536 sufficient information content.

537 In order to aid end users in extrapolating from colocation study performance to potential performance in a specific
538 application, performance metrics are often used. Although single value performance metrics do convey some
539 useful information about the agreement between the data from the measurement device being assessed and the
540 reference data, they can often be misleading in their evaluation of performance. This dictates a more rigorous and
541 empirical approach to data uncertainty assessment in order to determine if a measurement is fit for purpose. The
542 ability to assess device performance across the observed concentration range, as in the B-A and REU plots, enables
543 an end-user to make an informed decision about the capabilities of a measurement device in the target
544 concentration range. These visual tools also help identify any simple corrections that can be applied to improve
545 performance. In contrast, if an end-user was only provided with a single value metric, such as R^2 or RMSE then
546 it would be significantly more difficult to understand the likely implications of the measurement uncertainties.

547 All measurement devices suffer from errors, which result in deviations between the reported and true values.
548 These errors can come from a multitude of sources, with the scale of the deviation from the true value being
549 dependent on the nature of the error. Although a known measurement uncertainty for all applications would be
550 ideal for end users to be able to assess measurement device suitability for purpose, in many cases, especially for
551 LCS, this is not possible due to the presence of poorly characterised, or sometimes unknown, error sources. In the
552 absence of this, useful information on likely measurement performance can be obtained using colocation data

553 compared with a measurement with a quantified uncertainty. It is important that such a colocation study is carried
554 out in an environment as similar as possible to the application environment, as the unknown nature of many error
555 sources means their magnitude can change significantly between different locations and/or seasons (e.g. Fig. 6).
556 Ideally, depending on the measurement task, the user could use the colocation data to model the error causes and
557 use this to develop strategies to minimise final measurement uncertainty. Unfortunately, relevant colocation study
558 are often not available, and to generate the data would be prohibitively costly, which limits the user's ability to
559 make a realistic assessment of likely uncertainties. The presence of, often complex, error minimisation post
560 processing or calibration algorithms further complicates things. This additional uncertainty is most likely to bias
561 any performance prediction if the end user is unaware of the purpose or scale of the data corrections, and their
562 applicability to the target environmental conditions. Ideally, long term colocation data sets demonstrating the
563 performance of measurement hardware and software, in a range of relevant locations, over multiple seasons, and
564 carried out by impartial bodies would be available to inform measurement solution decisions.

565 In order for end users to take full advantage of the ever-increasing range of air pollution measurement devices
566 available, the questions being asked of the data must be commensurate with the information content of the data.
567 Ultimately this information content is determined by the measurement uncertainty. Thus, providing end users with
568 as accurate an estimate as possible of the likely measurement uncertainty, in any specific application, is essential
569 if end users are to be able to make informed decisions. Similarly, end users must specify the data uncertainty
570 requirements for each specific task if the correct tool for the job is to be identified. This requirement for air quality
571 management strategies to acknowledge the capabilities of available devices, both in the setting and monitoring of
572 limits, will only become increasingly important as target levels continue to decrease.

573 **Supplementary**

574 The supplement related to this article is available online at:

575 **Code and data availability**

576 The code and data for this study can be found on Zenodo: <https://zenodo.org/record/6518027#.YnKbH9PMJhE>.

577 The live code can be found on GitHub: <https://github.com/wacl-york/quant-air-pollution-measurement-errors>.

578 **Author contributions**

579 PE: Funding acquisition; Supervision. SD and PE: Project administration; Formal analysis. SD, PE & SL:
580 Conceptualization; Methodology; Investigation. SD & SL: Visualisation; Software. KR, NM, MF: Resources. SD,
581 SL, KR, NM, MF: Data curation. SD, PE, SL, TB, NM, TG & DH: Writing – review & editing.

582 **Competing interests**

583 The authors declare that they have no conflict of interest.

584 **Acknowledgements**

585 This work was funded as part of the UKRI Strategic Priorities Fund Clean Air program (NERC NE/T00195X/1),
586 with support from Defra. We would also thank the OSCA team (Integrated Research Observation System for

587 Clean Air) at the Manchester Air Quality Supersite (MAQS), for help in data collection for the regulatory-grade
588 instruments. The secondary research grade instruments used here (Thermo ozone 49i, 2B Technologies 202 ozone,
589 and Teledyne T200U NOx) are provided through the Atmospheric Measurement and Observation Facility
590 (AMOF) and the calibrations were carried out in the COZI Laboratory, a facility housed at the Wolfson
591 Atmospheric Chemistry Laboratories (WACL). Both funded through the National Centre for Atmospheric Science
592 (NCAS). Special thanks to Elena Martin Arenos, Chris Anthony, Killian Murphy, Stuart Young, Steve Andrews
593 and Jenny Hudson-Bell from WACL for the help and support to the project. Also, thanks to Stuart Murray and
594 Chris Rhodes from the Department of Chemistry Workshop for their technical assistance and advice. Thanks to
595 Andrew Gillah and Michael Golightly from the York Council who assisted with site access.

596

597 **References**

598 Altman, D. G. and Bland, J. M.: Measurement in Medicine: The Analysis of Method Comparison Studies, *J. R.*
599 *Stat. Soc. Ser. Stat.*, 32, 307–317, <https://doi.org/10.2307/2987937>, 1983.

600 Andrewes, P., Bullock, S., Turnbull, R., and Coolbear, T.: Chemical instrumental analysis versus human
601 evaluation to measure sensory properties of dairy products: What is fit for purpose?, *Int. Dairy J.*, 121,
602 105098, <https://doi.org/10.1016/j.idairyj.2021.105098>, 2021.

603 Bagkis, E., Kassandra, T., Karteris, M., Karteris, A., and Karatzas, K.: Analyzing and Improving the Performance
604 of a Particulate Matter Low Cost Air Quality Monitoring Device, *Atmosphere*, 12, 251,
605 <https://doi.org/10.3390/atmos12020251>, 2021.

606 Baldauf, R., Watkins, N., Heist, D., Bailey, C., Rowley, P., and Shores, R.: Near-road air quality monitoring:
607 Factors affecting network design and interpretation of data, *Air Qual. Atmosphere Health*, 2, 1–9,
608 <https://doi.org/10.1007/s11869-009-0028-0>, 2009.

609 Bigi, A., Mueller, M., Grange, S. K., Ghermandi, G., and Hueglin, C.: Performance of NO,
610 NO₂; low cost sensors and three calibration approaches within a real world
611 application, *Atmospheric Meas. Tech.*, 11, 3717–3735, <https://doi.org/10.5194/amt-11-3717-2018>, 2018.

612 Broday, D. M.: Wireless Distributed Environmental Sensor Networks for Air Pollution Measurement—The
613 Promise and the Current Reality, *Sensors*, 17, 2263, <https://doi.org/10.3390/s17102263>, 2017.

614 Brown, R. J. C., Hood, D., and Brown, A. S.: On the Optimum Sampling Time for the Measurement of Pollutants
615 in Ambient Air, *J. Autom. Methods Manag. Chem.*, 2008, 814715, <https://doi.org/10.1155/2008/814715>,
616 2008.

617 Castell, N., Dauge, F. R., Schneider, P., Vogt, M., Lerner, U., Fishbain, B., Broday, D., and Bartonova, A.: Can
618 commercial low-cost sensor platforms contribute to air quality monitoring and exposure estimates?,
619 *Environ. Int.*, 99, 293–302, <https://doi.org/10.1016/j.envint.2016.12.007>, 2017.

620 CEN/TS 17660-1: 2021, Air quality – Performance evaluation of air quality sensor systems – Part 1 Gaseous
621 pollutants in ambient air.
622 [https://standards.cen.eu/dyn/www/f?p=204:110:0:::FSP_PROJECT,FSP_LANG_ID:60880,25&cs=1B](https://standards.cen.eu/dyn/www/f?p=204:110:0:::FSP_PROJECT,FSP_LANG_ID:60880,25&cs=1B6992D14C0BCD6D6333E555D297F1306)
623 [6992D14C0BCD6D6333E555D297F1306](https://standards.cen.eu/dyn/www/f?p=204:110:0:::FSP_PROJECT,FSP_LANG_ID:60880,25&cs=1B6992D14C0BCD6D6333E555D297F1306) (accessed on 15 January 2022). 2021.

624 Chai, T. and Draxler, R. R.: Root mean square error (RMSE) or mean absolute error (MAE)? – Arguments against
625 avoiding RMSE in the literature, *Geosci. Model Dev.*, 7, 1247–1250, [https://doi.org/10.5194/gmd-7-](https://doi.org/10.5194/gmd-7-1247-2014)
626 [1247-2014](https://doi.org/10.5194/gmd-7-1247-2014), 2014.

627 Cordero, J. M., Borge, R., and Narros, A.: Using statistical methods to carry out in field calibrations of low cost
628 air quality sensors, *Sens. Actuators B Chem.*, 267, 245–254, <https://doi.org/10.1016/j.snb.2018.04.021>,
629 2018.

630 De Vito, S., Esposito, E., Castell, N., Schneider, P., and Bartonova, A.: On the robustness of field calibration for
631 smart air quality monitors, *Sens. Actuators B Chem.*, 310, 127869,
632 <https://doi.org/10.1016/j.snb.2020.127869>, 2020.

633 Doğan, N. Ö.: Bland-Altman analysis: A paradigm to understand correlation and agreement, *Turk. J. Emerg. Med.*,
634 18, 139–141, <https://doi.org/10.1016/j.tjem.2018.09.001>, 2018.

635 Duvall, R. M., Long, R. W., Beaver, M. R., Kronmiller, K. G., Wheeler, M. L., and Szykman, J. J.: Performance
636 Evaluation and Community Application of Low-Cost Sensors for Ozone and Nitrogen Dioxide, *Sensors*,
637 16, 1698, <https://doi.org/10.3390/s16101698>, 2016.

638 Feenstra, B., Papapostolou, V., Hasheminassab, S., Zhang, H., Boghossian, B. D., Cocker, D., and Polidori, A.:
639 Performance evaluation of twelve low-cost PM_{2.5} sensors at an ambient air monitoring site, *Atmos.*
640 *Environ.*, 216, 116946, <https://doi.org/10.1016/j.atmosenv.2019.116946>, 2019.

641 Feinberg, S. N., Williams, R., Hagler, G., Low, J., Smith, L., Brown, R., Garver, D., Davis, M., Morton, M.,
642 Schaefer, J., and Campbell, J.: Examining spatiotemporal variability of urban particulate matter and
643 application of high-time resolution data from a network of low-cost air pollution sensors, *Atmos.*
644 *Environ.*, 213, 579–584, <https://doi.org/10.1016/j.atmosenv.2019.06.026>, 2019.

645 GDE. Guidance for the Demonstration of Equivalence of Ambient Air Monitoring Methods.
646 <https://ec.europa.eu/environment/air/quality/legislation/pdf/equivalence.pdf> (accessed on 20 Dec 2021).
647 2010.

648 Gerboles, M., Lagler, F., Rembges, D., and Brun, C.: Assessment of uncertainty of NO₂ measurements by the
649 chemiluminescence method and discussion of the quality objective of the NO₂ European Directive, *J.*
650 *Environ. Monit.*, 5, 529–540, <https://doi.org/10.1039/B302358C>, 2003.

651 Giordano, M. R., Malings, C., Pandis, S. N., Presto, A. A., McNeill, V. F., Westervelt, D. M., Beekmann, M., and
652 Subramanian, R.: From low-cost sensors to high-quality data: A summary of challenges and best

653 practices for effectively calibrating low-cost particulate matter mass sensors, *J. Aerosol Sci.*, 158,
654 105833, <https://doi.org/10.1016/j.jaerosci.2021.105833>, 2021.

655 Gramsch, E., Oyola, P., Reyes, F., Vásquez, Y., Rubio, M. A., Soto, C., Pérez, P., Moreno, F., and Gutiérrez, N.:
656 Influence of Particle Composition and Size on the Accuracy of Low Cost PM Sensors: Findings From
657 Field Campaigns, *Front. Environ. Sci.*, 9, 2021.

658 Grégis, F.: On the meaning of measurement uncertainty, *Measurement*, 133, 41–46,
659 <https://doi.org/10.1016/j.measurement.2018.09.073>, 2019.

660 Hofman, J., Nikolaou, M., Shantharam, S. P., Stroobants, C., Weijs, S., and La Manna, V. P.: Distant calibration
661 of low-cost PM and NO₂ sensors; evidence from multiple sensor testbeds, *Atmospheric Pollut. Res.*, 13,
662 101246, <https://doi.org/10.1016/j.apr.2021.101246>, 2022.

663 JCGM. International vocabulary of metrology - Basic and general concepts and associated terms.
664 [https://www.bipm.org/documents/20126/2071204/JCGM_200_2012.pdf/f0e1ad45-d337-bbeb-53a6-](https://www.bipm.org/documents/20126/2071204/JCGM_200_2012.pdf/f0e1ad45-d337-bbeb-53a6-15fe649d0ff1?version=1.15&t=1641292389029&download=true)
665 [15fe649d0ff1?version=1.15&t=1641292389029&download=true](https://www.bipm.org/documents/20126/2071204/JCGM_200_2012.pdf/f0e1ad45-d337-bbeb-53a6-15fe649d0ff1?version=1.15&t=1641292389029&download=true) (accessed on 20 Dec 2021). 2012.

666 Jiao, W., Hagler, G., Williams, R., Sharpe, R., Brown, R., Garver, D., Judge, R., Caudill, M., Rickard, J., Davis,
667 M., Weinstock, L., Zimmer-Dauphinee, S., and Buckley, K.: Community Air Sensor Network
668 (CAIRSENSE) project: evaluation of low-cost sensor performance in a suburban environment in the
669 southeastern United States, *Atmospheric Meas. Tech.*, 9, 5281–5292, [https://doi.org/10.5194/amt-9-](https://doi.org/10.5194/amt-9-5281-2016)
670 [5281-2016](https://doi.org/10.5194/amt-9-5281-2016), 2016.

671 Karagulian, F., Barbieri, M., Kotsev, A., Spinelle, L., Gerboles, M., Lagler, F., Redon, N., Crunaire, S., and
672 Borowiak, A.: Review of the Performance of Low-Cost Sensors for Air Quality Monitoring, *Atmosphere*,
673 10, 506, <https://doi.org/10.3390/atmos10090506>, 2019.

674 Kirkham, H., Riepnicks, A., Albu, M., and Laverty, D.: The nature of measurement, and the true value of a
675 measured quantity, in: 2018 IEEE International Instrumentation and Measurement Technology
676 Conference (I2MTC), 2018 IEEE International Instrumentation and Measurement Technology
677 Conference (I2MTC), 1–6, <https://doi.org/10.1109/I2MTC.2018.8409771>, 2018.

678 Lewis, A. and Edwards, P.: Validate personal air-pollution sensors, *Nat. News*, 535, 29,
679 <https://doi.org/10.1038/535029a>, 2016.

680 Makar, P. A., Stroud, C., Akingunola, A., Zhang, J., Ren, S., Cheung, P., and Zheng, Q.: Vehicle-induced
681 turbulence and atmospheric pollution, *Atmospheric Chem. Phys.*, 21, 12291–12316,
682 <https://doi.org/10.5194/acp-21-12291-2021>, 2021.

683 Malings, C., Tanzer, R., Haurlyliuk, A., Kumar, S. P. N., Zimmerman, N., Kara, L. B., Presto, A. A., and R.
684 Subramanian: Development of a general calibration model and long-term performance evaluation of low-
685 cost sensors for air pollutant gas monitoring, *Atmospheric Meas. Tech.*, 12, 903–920,
686 <https://doi.org/10.5194/amt-12-903-2019>, 2019.

687 Mari, L., Wilson, M., and Maul, A.: Measurement across the Sciences: Developing a Shared Concept System for
688 Measurement, Springer International Publishing, Cham, <https://doi.org/10.1007/978-3-030-65558-7>,
689 2021.

690 Masson, N., Piedrahita, R., and Hannigan, M.: Approach for quantification of metal oxide type semiconductor gas
691 sensors used for ambient air quality monitoring, *Sens. Actuators B Chem.*, 208, 339–345,
692 <https://doi.org/10.1016/j.snb.2014.11.032>, 2015.

693 Mead, M. I., Popoola, O. A. M., Stewart, G. B., Landshoff, P., Calleja, M., Hayes, M., Baldovi, J. J., McLeod, M.
694 W., Hodgson, T. F., Dicks, J., Lewis, A., Cohen, J., Baron, R., Saffell, J. R., and Jones, R. L.: The use of
695 electrochemical sensors for monitoring urban air quality in low-cost, high-density networks, *Atmos.
696 Environ.*, 70, 186–203, <https://doi.org/10.1016/j.atmosenv.2012.11.060>, 2013.

697 Molina, M. J. and Molina, L. T.: Megacities and Atmospheric Pollution, *J. Air Waste Manag. Assoc.*, 54, 644–
698 680, <https://doi.org/10.1080/10473289.2004.10470936>, 2004.

699 Morawska, L., Thai, P., Liu, X., Asumadu-Sakyi, A., Ayoko, G., Bartonova, A., Bedini, A., Chai, F., Christensen,
700 B., Dunbabin, M., Gao, J., Hagler, G., Jayaratne, R., Kumar, P., Lau, A., Louie, P., Mazaheri, M., Ning,
701 Z., Motta, N., Mullins, B., Rahman, M., Ristovski, Z., Shafiei, M., Tjondronegoro, D., Westerdahl, D.,
702 and Williams, R.: Applications of low-cost sensing technologies for air quality monitoring and exposure
703 assessment: How far have they gone?, *Environ. Int.*, 116, 286–299,
704 <https://doi.org/10.1016/j.envint.2018.04.018>, 2018.

705 Mueller, M., Meyer, J., and Hueglin, C.: Design of an ozone and nitrogen dioxide sensor unit and its long-term
706 operation within a sensor network in the city of Zurich, *Atmospheric Meas. Tech.*, 10, 3783–3799,
707 <https://doi.org/10.5194/amt-10-3783-2017>, 2017.

708 Peters, D. R., Popoola, O. A. M., Jones, R. L., Martin, N. A., Mills, J., Fonseca, E. R., Stidworthy, A., Forsyth,
709 E., Carruthers, D., Dupuy-Todd, M., Douglas, F., Moore, K., Shah, R. U., Padilla, L. E., and Alvarez, R.
710 A.: Evaluating uncertainty in sensor networks for urban air pollution insights, *Gases/In Situ
711 Measurement/Validation and Intercomparisons*, <https://doi.org/10.5194/amt-2021-210>, 2021.

712 Popoola, O. A. M., Stewart, G. B., Mead, M. I., and Jones, R. L.: Development of a baseline-temperature
713 correction methodology for electrochemical sensors and its implications for long-term stability, *Atmos.
714 Environ.*, 147, 330–343, <https://doi.org/10.1016/j.atmosenv.2016.10.024>, 2016.

715 Rai, A. C., Kumar, P., Pilla, F., Skouloudis, A. N., Di Sabatino, S., Ratti, C., Yasar, A., and Rickerby, D.: End-
716 user perspective of low-cost sensors for outdoor air pollution monitoring, *Sci. Total Environ.*, 607–608,
717 691–705, <https://doi.org/10.1016/j.scitotenv.2017.06.266>, 2017.

718 Sayer, A. M., Govaerts, Y., Kolmonen, P., Lipponen, A., Luffarelli, M., Mielonen, T., Patadia, F., Popp, T., Povey,
719 A. C., Stebel, K., and Witek, M. L.: A review and framework for the evaluation of pixel-level uncertainty
720 estimates in satellite aerosol remote sensing, *Atmospheric Meas. Tech.*, 13, 373–404,
721 <https://doi.org/10.5194/amt-13-373-2020>, 2020.

- 722 Spinelle, L., Gerboles, M., Villani, M. G., Aleixandre, M., and Bonavitacola, F.: Field calibration of a cluster of
723 low-cost available sensors for air quality monitoring. Part A: Ozone and nitrogen dioxide, *Sens.*
724 *Actuators B Chem.*, 215, 249–257, <https://doi.org/10.1016/j.snb.2015.03.031>, 2015.
- 725 Sun, L., Westerdahl, D., and Ning, Z.: Development and Evaluation of A Novel and Cost-Effective Approach for
726 Low-Cost NO₂ Sensor Drift Correction, *Sensors*, 17, E1916, <https://doi.org/10.3390/s17081916>, 2017.
- 727 Thompson, M. and Ellison, S. L. R.: A review of interference effects and their correction in chemical analysis
728 with special reference to uncertainty, *Accreditation Qual. Assur.*, 10, 82–97,
729 <https://doi.org/10.1007/s00769-004-0871-5>, 2005.
- 730 Tian, Y., Nearing, G. S., Peters-Lidard, C. D., Harrison, K. W., and Tang, L.: Performance Metrics, Error
731 Modeling, and Uncertainty Quantification, *Mon. Weather Rev.*, 144, 607–613,
732 <https://doi.org/10.1175/MWR-D-15-0087.1>, 2016.
- 733 Williams, D. E.: Electrochemical sensors for environmental gas analysis, *Curr. Opin. Electrochem.*, 22, 145–153,
734 <https://doi.org/10.1016/j.coelec.2020.06.006>, 2020.
- 735 World Health Organization: WHO global air quality guidelines: particulate matter (PM_{2.5} and PM₁₀), ozone,
736 nitrogen dioxide, sulfur dioxide and carbon monoxide: executive summary, World Health Organization,
737 Geneva, 10 pp., 2021.
- 738 van Zoest, V., Osei, F. B., Stein, A., and Hoek, G.: Calibration of low-cost NO₂ sensors in an urban air quality
739 network, *Atmos. Environ.*, 210, 66–75, <https://doi.org/10.1016/j.atmosenv.2019.04.048>, 2019.
- 740 Yatkin, S., Gerboles, M., Borowiak, A., Davila, S., Spinelle, L., Bartonova, A., Dauge, F., Schneider, P., Van
741 Poppel, M., Peters, J., Matheussen, C., and Signorini, M.: Modified Target Diagram to check
742 compliance of low-cost sensors with the Data Quality Objectives of the European air quality directive,
743 *Atmos. Environ.*, 273, 118967, <https://doi.org/10.1016/j.atmosenv.2022.118967>, 2022.
- 744 Zucco, M., Curci, S., Castrofino, G., and Sassi, M. P.: A comprehensive analysis of the uncertainty of a
745 commercial ozone photometer, *Meas. Sci. Technol.*, 14, 1683–1689, [https://doi.org/10.1088/0957-](https://doi.org/10.1088/0957-0233/14/9/320)
746 [0233/14/9/320](https://doi.org/10.1088/0957-0233/14/9/320), 2003.